Partial tuning of motor cortex neurons to final posture in a free-moving paradigm

Tyson N. Aflalo and Michael S. A. Graziano*

Department of Psychology, Princeton University, Princeton, NJ 08544

Motor cortex neurons in the monkey brain were tested with a diverse and naturalistic arm movement set. Over this global set of movements, the neurons showed a limited but significant degree of tuning to the multijoint posture attained by the arm at the end of each movement. Further supporting the hypothesis that the neurons are partially tuned to end posture, the postures preferred by the neurons significantly matched the postures evoked by electrical stimulation of the same cortical sites. However, much of the variance in neuronal activity remained unexplained even by the end-posture model, and thus other variables must have contributed to the response profile of the neurons. One possibility is that motor cortex neurons become tuned to the wide variety of movement parameters that are relevant to the animal's normal behavioral repertoire, and, therefore, any one parameter accounts for only a limited amount of neuronal variance.

direction tuning | microstimulation | primary motor cortex

How do neurons in motor cortex encode movement? Georgopoulos and colleagues (1, 2) studied monkeys performing a reaching task and found that each neuron was tuned to a preferred direction of reach. Subsequent studies suggested that direction tuning is only one part of a more complex tuning function. For most neurons, when the initial position of the hand was shifted to different parts of the workspace, or when the posture of the arm was altered, the preferred direction changed (3–5). Thus, a single preferred direction could not account for the behavior of the neurons, and other variables such as joint angle and arm posture must have contributed. Neural correlates have been found for a range of variables including force, static hand position, distance, speed, curvature of hand path, joint angle, and muscle activity (6–17). It seems increasingly likely that the neurons are tuned to combinations of movement parameters that are of use to the animal.

One limitation of these previous experiments in exploring the complexity of neuronal tuning is that they typically used a restricted, simplified movement set, such as a set of reach directions, a set of directions of isometric force on a lever, a set of hand movements confined to a 2D plane, or a directional movement of the wrist. This restriction on the movement set limits the kinds of neuronal responses and tuning functions that can be obtained. Models of neuronal tuning that fit the data well in a restricted condition may not account for much of the neuronal behavior in a more naturalistic condition.

Here we examined neuronal activity in primary motor cortex of two monkeys while simultaneously measuring eight degrees of freedom of the arm. The monkey moved its limb freely, reaching for pieces of fruit, manipulating objects, putting items in its mouth, scratching and grooming itself, and engaging in other spontaneous behavior. After recording neuronal activity during this varied movement set, we tested the extent to which the firing of each neuron could be explained by (*i*) a preferred direction of the hand through space, (*ii*) a preferred end point of the hand in space, and (*iii*) a preferred, multijoint end posture of the arm.

Electrical stimulation of motor cortex can cause the arm to move to a specific, complex posture typically involving many joints (18–20). We therefore also compared the response prop-erties of neurons to the postures evoked by stimulation of the same cortical site to determine whether there was a significant match.

Results

Direction Tuning. Fig. 1*A* shows a front view of a set of 683 hand movements made by the monkey over 15 min. As described in greater detail in the supporting information, which is published on the PNAS web site, movements were individuated on the basis of the distinctive rising and falling speed profile of the hand. As shown in Fig. 1*A*, the movements densely sampled a large portion of the space around the monkey. Details of the degree of curvature of movements, mean length, mean speed, range of different directions, and extent of the workspace covered are given in the supporting information.

During these movements we recorded from a neuron in primary motor cortex, and a mean firing rate for the neuron was computed for each movement. As detailed in the supporting information, the neuron was located in the arm and hand representation in primary motor cortex, in which most neurons (89%) responded significantly in relation to simple movement of the shoulder or elbow.

In the preferred direction model (1, 2) a neuron fires most during hand movement in a particular, preferred direction. The firing rate is proportional to the cosine of the angle between the actual hand direction and the preferred hand direction. A regression analysis (see supporting information) was used to obtain the preferred direction that best fit the neuronal data and to obtain an R^2 value indicating how much of the variance in neuronal activity could be attributed to the cosine tuning to the preferred direction. Fig. 1*B* shows the cosine fit to the data for this example neuron. The R^2 value is 0.03, indicating that the direction tuning model accounted for almost none of the variance in neuronal activity. Sixty-three neurons were tested in this fashion. The black bars in Fig. 2*A* show the distribution of R^2 values for all neurons. Almost all values were <0.1. The direction tuning model explained almost none of the variance in the sample of neurons. These results do not show that neurons in motor cortex are not direction-tuned. Rather, they show that, during free movement, when many movement parameters presumably contribute to the activity of neurons, direction tuning makes a vanishingly small contribution.

Neurons in motor cortex have a consistent preferred direction when tested on a center-out task (1, 2). Changing the start position of the hand or the start posture of the arm, however, can alter the preferred direction (3–5). In our study, the lack of a clear preferred direction might have resulted from our use of a diverse movement set including a variety of start positions. To test this hypothesis we analyzed a restricted subset of the movements that more closely resembled a center-out task. Fig. 1*C* shows selected movements from Fig. 1*A* that originated
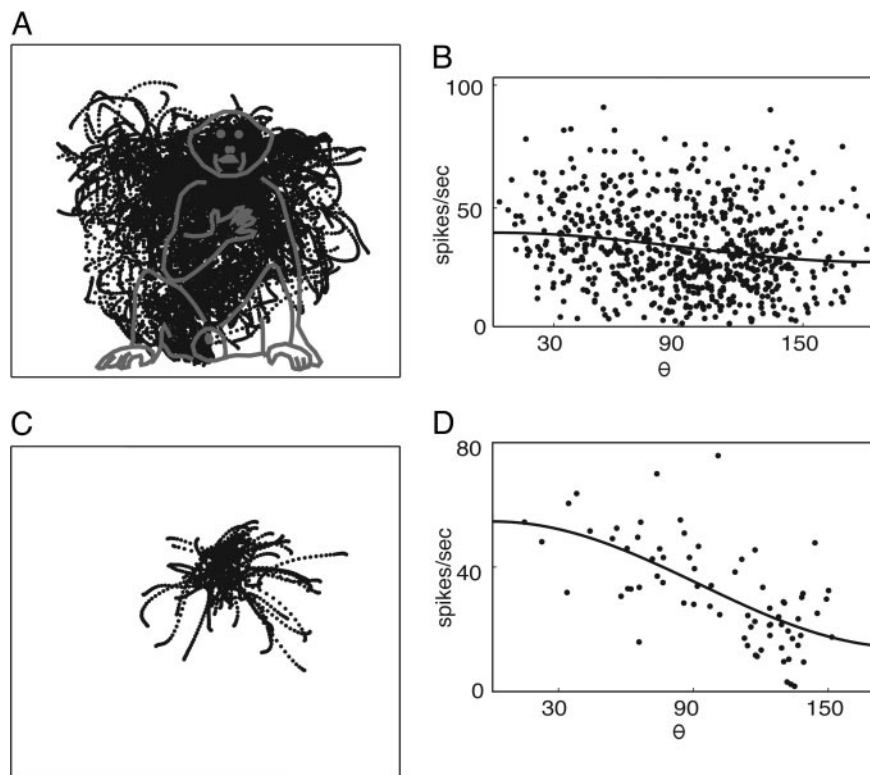
NEUROSCIENCE

Fig. 1. Example of a motor cortex neuron that is locally but not globally direction tuned. (*A*) Front view of 683 hand movements made during 15 min. Each trail of dots represents one movement measured at 14.3-ms intervals. The monkey drawing shows the approximate scale and location of the animal. (*B*) Firing rate of the neuron during each movement vs. angular deviation ($\Delta\theta$) between movement vector and preferred vector. Fit line is cosine fit. $R^2 = 0.03$; $P > 0.05$. (*C*) Seventy-three selected movements that originated within a 5-cm radius sphere and were between 6 and 15 cm in length. (*D*) Direction tuning over the limited movement set. $R^2 = 0.40$; $P < 0.0001$.

within a 5-cm radius sphere and that were between 6 and 15 cm in length. Fig. 1*D* shows the cosine tuning of the example neuron over this subset. The cosine fit has an R^2 value of 0.40 ($P < 0.0001$). Thus, over the limited movement set, a significant component of direction tuning can be extracted, accounting for ≈40% of the neuron's variance.

As shown in Fig. 2*A* for the population of neurons, the limited movement set had a significantly higher distribution of R^2 values than the unrestricted movement set ($F = 192.00$; $P < 0.0001$). Tuning to a single preferred direction can therefore account for much of the behavior of the neurons over a restricted movement set, but not over a complete movement set. The neurons appeared to be locally but not globally direction-tuned.

End-Point Tuning. What tuning function, if any, might account for a cell's global behavior across a full range of movements? If a cell is end-point-tuned, then it should fire most during movements that end with the hand near a preferred point in space. It should fire less during movements that end with the hand far from that preferred point. To test for end-point tuning, we modeled the firing rate of the neuron as a Gaussian function of end point, in which the Gaussian was peaked at a preferred spatial location (see supporting information). For each neuron, we obtained an R^2 value indicating how well this end-point model fit the neuronal data. Fig. 2*B* shows the distribution of R^2 values for the population of neurons. The R^2 values were slightly higher for the preferred end-point model than for the preferred direction model. However, neither model accounted for much of the variance. For more than half of the neurons, the R^2 value was <0.1.

End-Posture Tuning. Electrical stimulation of sites in motor cortex can evoke movement of the arm to a specific final joint config-

uration or posture (18–20). We therefore tested whether the neurons were tuned to the end posture of a movement. Eight degrees of freedom of the arm were monitored, including grip aperture and seven joint angles. These degrees of freedom define an 8D posture space. We modeled neuronal firing rate as a Gaussian surface in 8D space whose peak corresponds to the preferred end posture. Movements that terminate at a posture near the peak of the Gaussian should be associated with a high neuronal firing rate, and movements that terminate at a posture far from the peak of the Gaussian should be associated with a low neuronal firing rate. For each neuron, we obtained an R^2 value indicating how well this model fit the neuronal data. The distribution of R^2 values across the population of neurons was significantly higher for the end-posture model than for the end-point model or the direction model (see Fig. 2*B*; $F = 63.71$; $P < 0.0001$). However, much of the variance remained unexplained even by the end-posture model. These results therefore do not show that neurons in motor cortex are primarily end-posture-tuned. Rather, they show that, during free movement, when many movement parameters presumably contribute to the activity of neurons, end-posture tuning makes a significant contribution. It is important to note that even a relatively small R^2 value can represent a statistically significant contribution to the total but suggests that other factors also contribute.

In a second variant to end-posture tuning, in addition to considering the final posture of each movement, we considered the trajectory of the movement through 8D posture space. In this posture-plus-trajectory model, if the movement is aimed directly at the preferred posture, the neuron should fire more, and if the movement is aimed away from the preferred posture, the neuron should fire less, with firing rate proportional to the cosine of the
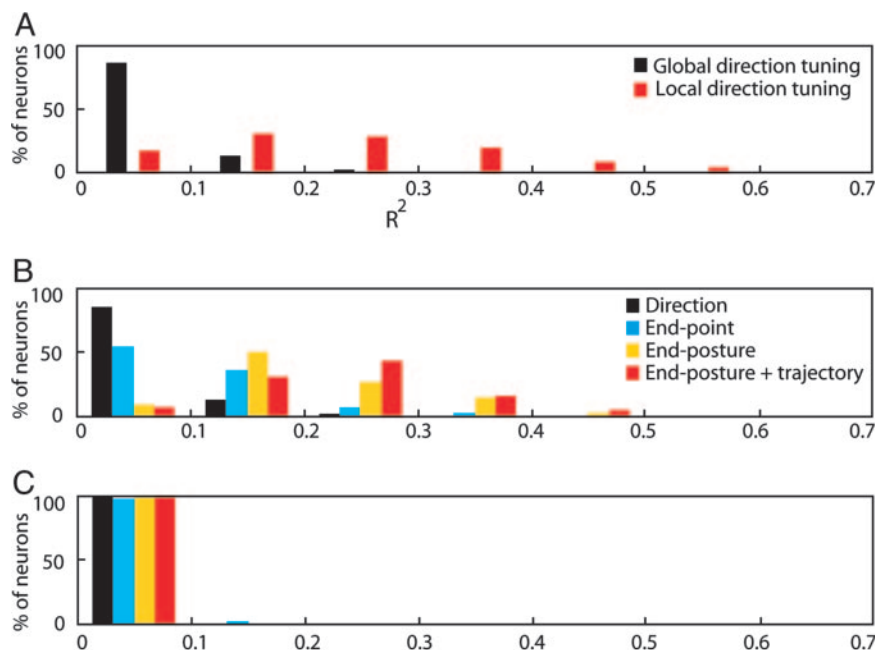
Fig. 2. Group data comparing different models of neuronal tuning. (*A*) Direction tuning on a complete movement set (global) resulted in low R^2 values for most neurons; direction tuning on a limited movement set (local) resulted in significantly higher R^2 values (ANOVA, $F = 192.00$, $P < 0.0001$). (*B*) Comparison of four models tested on the complete movement set. The four distributions of R^2 values are significantly different (ANOVA, $F = 63.71$, $P < 0.0001$). (*C*) Same four models as in *B* but applied to randomized data. The four distributions of R^2 values are not significantly different ($F = 0.92$; $P = 0.43$).

angular error (see supporting information). Using this directional factor as an additional regressor, we obtained R^2 values that were slightly higher than for the end-posture model alone. Thus, of the models of neuronal tuning tested here, the one that accounted for the largest fraction of neuronal behavior over the global range of movement was an end-posture model in which each neuron fired most during movements that (*i*) were aimed toward the preferred posture and (*ii*) terminated near the preferred posture.

The different models of neuronal tuning involved different analysis steps and different numbers of regressors. One possibility is that models with more regressors might be inherently able to extract higher R^2 values, regardless of the actual manner in which the neurons are tuned. We addressed this concern in three ways. First, and most directly, we used an R^2 value that was corrected for the number of regressors (21). In theory this method corrects for the potential statistical bias.

Second, we analyzed a randomized data set using the same models. The data set included the same movements, but the firing rates assigned to the movements were randomized. Will the models with a greater number of regressors be able to extract higher R^2 values from this noise, thus demonstrating that the number of regressors *per se* was a significant factor in the results? As shown in Fig. 2*C*, the R^2 values were near zero and the different models were not significantly different from each other ($F = 0.92$; $P = 0.43$).

Third, we created artificial neurons that were tuned to a specific direction of the hand, to a specific final location of the hand, or to a specific final posture of the arm. The data for these artificial neurons contained an actual, recorded movement set, but the firing rate of each neuron was artificially generated according to the three fitting functions, with randomized noise added. An artificial direction-tuned neuron is expected to show a high R^2 value when tested on a direction-tuned model. But will the end-point model and the end-posture model, with their greater number of regressors, extract an even higher R^2 value from the artificial direction-tuned neuron? As detailed in the

supporting information, an artificial neuron that was direction-tuned showed a high R^2 value only when tested on the directional model and showed a near zero R^2 value when tested on the end-point or end-posture models. Similarly, an artificial neuron that was end-point-tuned and an artificial neuron that was end-posture-tuned showed high R^2 values only when tested on their appropriate regression models. In this test on the artificial neurons, the analysis technique correctly identified each neuron's tuning function. In particular, the models that had greater numbers of regressors did not simply extract higher R^2 values from all neurons regardless of their tuning, but rather extracted high R^2 values from neurons appropriately tuned to the model being tested.

Comparison Between Neurons and Stimulation. Fig. 3*A* shows data from an example neuron. First the end-posture tuning was found by using the regression analysis described above. This analysis obtained a Gaussian surface in 8D posture space for which the peak of the Gaussian corresponded to the neuron's preferred posture. In this graph, the *x* axis represents the distance in posture space between the final posture of each movement and the preferred posture of the neuron. It is important to note that this distance is not the distance of the hand from a preferred location in space, but rather the distance of the arm from a preferred configuration in posture space. Thus, the units cannot be in Cartesian centimeters. Instead, we have expressed the units in standard deviations of the Gaussian fitting function. In this fashion, all eight dimensions of posture space can be expressed in the same units, and a 1D graph can be presented. The advantage of the 1D graph is that it shows the Gaussian fit to the data: on average, movements that terminated near the preferred posture (within a standard deviation of the peak of the Gaussian) had higher firing rates, and movements that terminated progressively farther from the preferred posture had progressively lower firing rates. Approximately 40% of this neuron's variance was attributable to the Gaussian tuning to the preferred posture
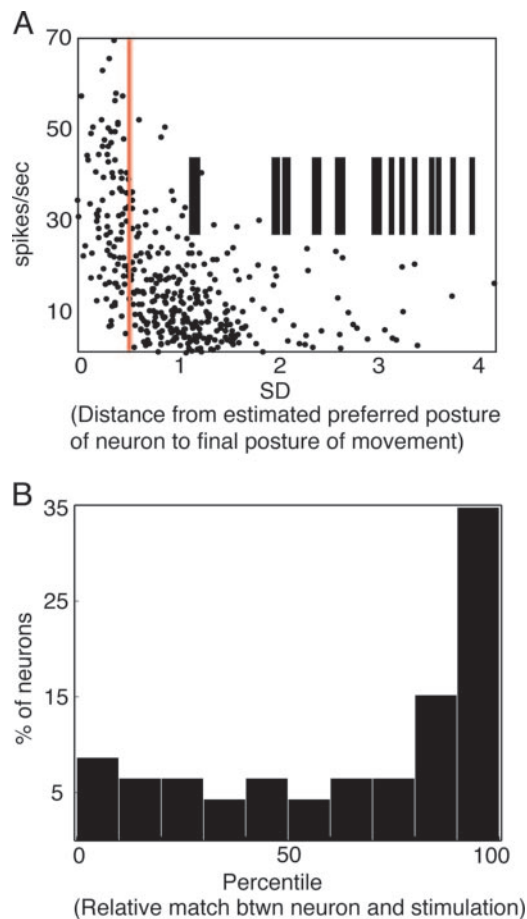
Fig. 3. Comparison of neuronal tuning and stimulation-evoked postures. (*A*) Data from an example neuron. The preferred final posture was determined by regression analysis. The final posture of each movement was compared to the preferred posture. The distance between them was calculated in 8D posture space. Distance was measured in units of standard deviations of the Gaussian tuning function to express all eight dimensions in posture space in equivalent units. This distance is plotted on the *x* axis, and firing rate during the movement is plotted on the *y* axis. The data fit the Gaussian tuning function with an R^2 value of 0.38 ($P < 0.0001$). Electrical stimulation of the same cortical site evoked a final posture. The mean stimulation-evoked posture is plotted (red vertical line) and was near the preferred posture of the neuron. The mean stimulation-evoked postures from other cortical sites (black vertical bars) were farther from the preferred posture of this neuron. (*B*) For each neuron a percentile was computed indicating how closely the neuron's preferred posture matched the posture evoked by stimulation of the same cortical site as compared to stimulation of other cortical sites. This distribution is not uniform; it is significantly greater than 50% (binomial test, $P < 0.0001$).

($R^2 = 0.38$; $P < 0.0001$). (Additional group data on neuronal tuning to end posture are given in the supporting information.)

After recording from this neuron, before withdrawing the electrode, we electrically stimulated the same site in cortex with a 500-ms train of biphasic pulses (0.2 ms per phase, negative phase leading, 200 Hz, 50 μA), and the arm moved to a final posture. Such stimulation-evoked postures were detailed in a previous study (20). In the present example, data were collected from 30 stimulation trials, and the mean final posture was obtained. The red vertical line in Fig. 3*A* shows the location of this stimulation-evoked posture relative to the neuron's preferred posture. The stimulation-evoked posture was near the peak of the neuron's Gaussian tuning function, 0.4 SD away from the neuron's preferred posture.

The postures evoked at all other cortical sites tested are also shown on the same graph as vertical black lines. They are all farther from the neuron's preferred posture (>1 SD away from the preferred posture). Thus, the neuron's preferred posture matched best to the posture obtained on stimulation of the same cortical site and matched less well to postures obtained on stimulation of all other sites. This result shows a specific correspondence between the properties of the neuron and the results of stimulating the same site in cortex.

To parameterize this result, we ranked the concordant stimulation site (stimulation site at the same cortical location as the neuron) in comparison to the discordant stimulation sites (stimulation sites at different cortical locations from the neuron) in terms of how closely they matched the preferred posture of the neuron. For the example neuron in Fig. 3*A*, the concordant stimulation site ranked first, in the 90th-to-100th percentile range. For each neuron, we obtained a percentile in this fashion. If there was no overall match between neuron properties and stimulation results, then the percentiles should be randomly distributed between 0 and 100. If there was a match between neuron properties and stimulation results, then the percentiles should be skewed to the high end. As shown in the population data in Fig. 3*B*, the percentiles are not randomly distributed. They are skewed to the high end, with the distribution significantly above the 50th percentile (binomial test, $P < 0.0001$). Indeed, half of the neurons are above the 80th percentile.

These results indicate that there is a significant degree of match between the postures preferred by neurons as determined by the regression analysis and the postures evoked by electrical stimulation of the same sites in cortex. However, the match is not absolute, with neurons showing a range of other percentiles.

Discussion

Contribution of Different Types of Tuning to Overall Variance. In many experiments on motor cortex neurons, a movement set is used in which the direction of the hand in space is varied systematically among conditions (1, 2, 7–9). The speed and curvature of the reach and posture of the arm may vary naturally from trial to trial, but this variability is small in a trained monkey making stereotyped movements. Thus, the variance in neuronal firing rate can be ascribed mainly to the direction of the hand in space. Regression analysis can result in R^2 values that are >0.5 and sometimes as high as 0.9 (11). Such experiments ask whether direction tuning is statistically reliable when isolated. Other experiments have asked whether speed tuning (11), distance tuning (9), or hand position tuning (6) are statistically reliable when isolated.

The present experiment addressed a fundamentally different question. Given the "free movement" of the arm, in which many movement parameters are at play in a more naturalistic fashion, how much of the total neuronal variance can be attributed to direction tuning, tuning for a preferred hand location in space, or tuning for a preferred multijoint arm posture?

We found that direction tuning generally accounted for <10% of the variance in neuronal activity over the global movement set. Tuning to a preferred location of the hand in space also accounted for little of the variance. Tuning to a preferred posture of the arm accounted for significantly more of the variance. Because the postures preferred by the neurons showed a significant match to the postures evoked by electrical stimulation, the study provides evidence that neuronal tuning to final posture exists and plays a role in the control of movement.

However, the results also indicate that posture tuning is only one contributing source of variance in neuronal activity. The remainder of the variance is likely to be caused by a combination of movement and contextual variables such as hand speed (11), curvature of hand path (12), distance of movement (9), force (8, 15), and probably other variables.

Local vs. Global Direction Tuning. We found significant direction tuning over a limited movement set. This limited set resembled the more typically studied center-out paradigm in that the movements began from a central location and radiated outward in all directions for a limited distance. This finding of a more consistent direction tuning for the local movement set than for the global movement set is in agreement with experiments showing that a neuron's preferred direction changes when the starting position and posture of the arm are changed (3–5). In such experiments, the preferred direction rotates when the starting configuration of the arm is changed, and this alteration in preferred direction occurs in a direction and by an amount that are idiosyncratic and different from one starting configuration of the arm to the next and from one neuron to the next. A population average suggested that the preferred directions tend to rotate partially with the shoulder joint (3), but at the single neuron level the change in preferred direction is variable. Such results indicate that a neuron cannot be characterized by a single preferred direction. Our results are consistent with these previous findings, suggesting that cells are tuned to a preferred direction mainly locally and that a single preferred direction does not apply globally.

Distinction Between Posture and Hand Position. Previous studies examined neuronal activity when the hand moved to a single final position from multiple starting positions or when the hand applied isometric force toward particular locations in space (3, 5, 7). These studies did not find neuronal tuning to a goal hand position. It is worth noting that these studies generally looked at population averages. It is possible that motor cortex contains some neurons with some degree of tuning to goal hand positions that is lost in the population average. However, the results consistently show that tuning to a final hand position is at least not a prominent influence.

In the present study we tested whether neurons were tuned to a particular final hand position in space. The R^2 values were typically <0.1, indicating little tuning for goal hand positions. These results are consistent with previous work.

In our previous stimulation experiments (18–20) we found that electrical stimulation of a site in cortex tended to drive the hand to a specific final location regardless of starting location. This effect of stimulation at first appears to be at odds with the neuronal data. However, it is crucial to recognize the difference between arm posture and hand position. For example, upon stimulation of some sites the hand moved to the mouth and the mouth opened. Yet the stimulation did not merely specify a hand position; it specified an arm posture. There are many possible arm postures consistent with a hand location near the mouth, but the stimulation evoked a posture in which the elbow was in lower space, the shoulder was slightly internally rotated, the forearm was supinated, the wrist was straight, and the grip aperture was closed. This posture resembled the monkey's natural feeding posture. Are neurons in motor cortex tuned to complex postures of the arm? The present study shows that there is a significant degree of tuning to the final posture of a movement and that the postures preferred by neurons show a significant match to the postures obtained upon stimulation.

If neurons in motor cortex are tuned to a preferred posture, then why does this tuning not manifest itself in studies that test hand location in space? The arm contains so many degrees of joint rotation that posture space and hand position space do not correspond in a simple fashion. Note that two very different postures might involve similar hand locations in space and that two very different hand locations in space might involve similar postures that differ from each other only in the angle of one joint. Thus, it is unlikely that posture coding would be detected in studies that examine hand position and movement. As described in the supporting information, we constructed "artificial" neu-

rons tuned to specific postures. These neurons, when tested for tuning to a hand location in space, resulted in low R^2 values and no clear preference for hand location. Yet each of these artificial neurons was tuned to a posture, and the preferred posture was necessarily associated with a hand position in space. These results on the artificial neurons show particularly clearly how a posture-tuned neuron would go undetected in experiments that measure only hand position or hand movement. The entire configuration of the arm must be measured to detect posture tuning.

Partial Match Between Neurons and Stimulation. Our results show a significant degree of match between the postures preferred by neurons and postures evoked by electrical stimulation of the same cortical site. Yet the match is not absolute. The mismatch may have a variety of sources. First, many neurons in motor cortex may simply not be posture-tuned. Indeed, some of the neurons showed low R^2 values for posture tuning, <0.2. Second, even the neurons that are posture-tuned are noisy, and thus the estimate of their preferred posture may not be precise. Third, stimulation directly activates a ball of neighboring neurons that might have a diversity of properties; thus, stimulation may cause an averaging or summing of these properties. These sources of error are likely to have diluted the match between neuronal properties and stimulation effects.

It has long been known that stimulation is helpful in discovering basic motor or sensory properties encoded in cortex, especially because the technique is causal rather than correlational (22–26). But because of the limitations of the technique, especially the direct stimulation of nearby neurons with diverse properties, the strongest evidence is always provided by a convergence of different techniques on a similar answer. In the present case a convergence of stimulation effects and single-neuron properties strongly supports the hypothesis that motor cortex neurons control movement partly by specifying a final posture.

Partial Coding of Final Posture. Motor cortex neurons correlate with many movement parameters (1–17). It seems increasingly clear that tuning to a single movement parameter is too simple a model to account for the behavior of these neurons. Rather, the neurons appear to be tuned in a complex, multidimensional space, and some degree of tuning to specific parameters can be extracted from that multidimensional tuning profile. Given different tasks and different movement sets, different types of tuning are obtained.

In the past we suggested that the postures evoked by electrical stimulation of motor cortex might reflect a fundamentally posture-based strategy for movement control (19). Such posture-based control strategies, in which movements are coordinated by first determining the desired final posture and then planning the trajectory to that posture, have been proposed by many others (27–30). However, given the diversity of movements in the animal's repertoire, it seems unlikely that the motor cortex uses one control strategy. The present results suggest that, although motor cortex neurons include some degree of posture tuning, this type of tuning does not account for the full range of neuronal behavior, and other variables must be at play. The results are more consistent with the hypothesis that a posture-based control strategy is one part of a more diverse and complex movement control system. For example, a recent study has identified what may be partially segregated neuronal populations for maintaining a steady arm posture and controlling a directional arm movement (31).

Recently it has been proposed that the motor system uses an "optimal control" method (32, 33). In this hypothesis the system optimizes the control of task-relevant parameters, often leaving other parameters to vary. In one type of task, the relevant

parameter may be hand direction; in another task, the relevant parameter may be quite different, e.g., the final striking position of the head of a hammer. One suggestion, therefore, is that there is no single, preferred parameter (such as direction, speed, force, or end point) used for all tasks, but instead the parameters being specified by the optimal control strategy depend on the task being performed. Studies involving a directional reaching task might tend to reveal a directional control strategy, whereas studies involving more posture-based tasks might tend to reveal a more postural control strategy. We suggest that the reason why neurons in motor cortex show some degree of end-posture coding is that monkeys normally spend a high proportion of time maintaining specific, complex arm postures to stabilize and orient the hand during hand actions (34). In this hypothesis, the neuronal tuning reflects common aspects of the monkey's behavioral repertoire.

Methods

All procedures were approved by the Princeton University Institutional Animal Care and Use Committee and the attendant veterinarian and were in accordance with National Institutes of Health and U.S. Department of Agriculture guidelines. We studied two adult male *Macaca fascicularis*. Detailed methods are presented in the supporting information.

A varnish-coated tungsten microelectrode (Frederick Haer, impedance 0.5–2 MΩ) was used to obtain neural signals that were amplified (A-M Systems amplifier, model 1800) filtered (300–5,000 Hz), and recorded at 25,000 Hz. An offline spike-sorting algorithm was used to assign spikes to individual neurons. Typically one to three neurons could be reliably isolated on the electrode at one time.

At each cortical site, after recording neuronal activity, we tested the effect of electrical stimulation (Grass S88 stimulator and two SIU6 stimulus isolation units). Stimulation consisted of a 500-ms, 200-Hz train of biphasic pulses, each phase 0.2 ms in duration, negative phase leading. Current was measured by means of the voltage drop across a 1 KΩ resistor in series with the return lead of the stimulus isolation units. The current level was adjusted until a clear, consistent, multijoint movement of the arm was obtained, typically between 25 and 100 μA.

Detailed methods for measurement of arm movement are provided in the supporting information. Briefly, the 3D positions of points on the limb were measured by means of an Optotrak 3020 system (Northern Digital). This system tracked infrared light-emitting diodes that were taped to the monkey's hand and arm. Based on these tracking data, eight degrees of freedom were calculated: the elevation, azimuth, and internal/external rotation of the shoulder joint; the flexion of the elbow; pronation of the forearm; extension of the wrist; adduction of the wrist; and grip aperture.

The monkeys were not killed at the termination of this experiment; thus, the locations of the stimulation sites were reconstructed through nonhistological means. The central and arcuate sulci were located first by shining a bright light on the dura during the initial craniotomy surgery. Both sulci were clearly visible through the dura. The microdrive was mounted to the recording chamber, and the locations of the visualized sulci were measured with the tip of the guide tube. In this way, the locations of the sulci were obtained in microdrive coordinates.

During the daily experiments, the measured location of the central sulcus was confirmed to within 0.5 mm by recording and stimulating to either side of the sulcus. Just posterior to the sulcus, in primary somatosensory cortex, we observed the expected small tactile receptive fields on the contralateral arm and hand and also the expected lack of effect of electrical stimulation. Just anterior to the sulcus we obtained the expected low stimulation thresholds in primary motor cortex. The location of the arcuate sulcus was confirmed by stimulating just anterior to it and obtaining no skeletomotor movements, but instead stimulation-evoked saccadic eye movements. The location of both the central and arcuate sulci were further verified by using the pattern of cellular activity and silence obtained on long electrode penetrations to reconstruct the arrangement of cortex and white matter. The sites tested were located in the arm representation in motor cortex and were within the anterior bank of the central sulcus or on the cortical surface within 2 mm of the central sulcus. They therefore lay within the boundaries of traditional primary motor cortex. As detailed in the supporting information, a preliminary analysis indicated that 89% of the studied neurons responded significantly in relation to rotation of the shoulder or elbow joint, indicating that the neurons were in the correct portion of motor cortex. All neurons that were encountered by the electrode and that could be held long enough for collection of a full data set were included in the analysis.

1. Georgopoulos, A. P., Kalaska, J. F., Caminiti, R. & Massey, J. T. (1982) *J. Neurosci.* **2,** 1527–1537.
2. Georgopoulos, A. P., Schwartz, A. B. & Kettner, R. E. (1986) *Science* **233,** 1416–1419.
3. Caminiti, R., Johnson, P. B. & Urbano, A. (1990) *J. Neurosci.* **10,** 2039–2058.
4. Scott, S. H. & Kalaska, J. F. (1995) *J. Neurophysiol.* **73,** 2563–2567.
5. Sergio, L. E. & Kalaska, J. F. (2003) *J. Neurophysiol.* **89,** 212–228.
6. Georgopoulos, A. P., Caminiti, R. & Kalaska, J. F. (1984) *Exp. Brain Res.* **54,** 446–454.
7. Kettner, R. E., Schwartz, A. B. & Georgopoulos, A. P. (1998) *J. Neurosci.* **8,** 2938–2947.
8. Georgopoulos, A. P., Ashe, J., Smyrnis, N. & Taira, M. (1992) *Science* **256,** 1692–1695.
9. Fu, Q. G., Suarez, J. I. & Ebner, T. J. (1993) *J. Neurophysiol.* **70,** 2097–2116.
10. Ashe, J. & Georgopoulos, A. P. (1994) *Cereb. Cortex* **4,** 590–600.
11. Reina, G. A., Moran, D. W. & Schwartz, A. B. (2001) *J. Neurophysiol.* **85,** 2576–2589.
12. Hocherman, S. & Wise, S. P. (1991) *Exp. Brain Res.* **83,** 285–302.
13. Li, C. S., Padoa-Schioppa, C. & Bizzi, E. (2001) *Neuron* **30,** 593–607.
14. Kakei, S., Hoffman, D. & Strick, P. (1999) *Science* **285,** 2136–2139.
15. Evarts, E. V. (1968) *J. Neurophysiol.* **31,** 14–27.
16. Cheney, P. D., Fetz, E. E. & Palmer, S. S. (1985) *J. Neurophysiol.* **53,** 805–820.
17. Holdefer, R. N. & Miller, L. E. (2002) *Exp. Brain Res.* **146,** 233–243.
18. Graziano, M. S. A., Taylor, C. S. R. & Moore, T. (2002) *Neuron* **34,** 841–851.
19. Graziano, M. S. A., Taylor, C. S. R., Moore, T. & Cooke, D. F. (2002) *Neuron* **36,** 349–362.
20. Graziano, M. S. A., Aflalo, T. & Cooke, D. F. (2005) *J. Neurophysiol.* **94,** 4209–4223.
21. Cohen, J., Cohen, P., West, S. G. & Aiken, L. S. (2003) *Applied Multiple Regression/Correlation Analysis for the Behavioral Sciences* (Lawrence Erlbaum Associates, Mahwah, NJ), 3rd Ed.
22. Robinson, D. A. & Fuchs, A. F. (1969) *J. Neurophysiol.* **32,** 637–648.
23. Bruce, C. J., Goldberg, M. E., Bushnell, M. C. & Stanton, G. B. (1985) *J. Neurophysiol.* **54,** 14–734.
23. Tehovnik, E. J. & Lee, K. (1993) *Exp. Brain Res.* **96,** 430–442.
24. Stepniewska, I., Fang, P. C. & Kaas, J. H. (2005) *Proc. Natl. Acad. Sci. USA* **102,** 4878–4883.
26. Salzman, C. D., Britten, K. H. & Newsome, W. T. (1990) *Nature* **346,** 174–177.
27. Desmurget, M. & Prablanc, C. (1997) *J. Neurophysiol.* **77,** 452–464.
28. Feldman, A. G. (1986) *J. Mot. Behav.* **18,** 17–54.
29. Giszter, S. F., Mussa-Ivaldi, F. A. & Bizzi, E. (1993) *J. Neurosci.* **13,** 467–491.
30. Rosenbaum, D. A., Loukopoulos, L. D., Meulenbroek, R. G., Vaughan, J. & Engelbrecht, S. E. (1995) *Psychol. Rev.* **102,** 28–67.
31. Kurtzer, I., Herter, T. M. & Scott, S. H. (2005) *Nat. Neurosci.* **8,** 498–504.
32. Scott, S. H. (2004) *Nat. Rev. Neurosci.* **5,** 532–546.
33. Todorov, E. & Jordon, M. I. (2002) *Nat. Neurosci.* **5,** 1226–1235.
34. Graziano, M. S. A., Cooke, D. F., Taylor, C. S. R. & Moore, T. (2003) *Exp. Brain Res.* **155,** 30–36.

Supporting Text

Note on R^2 values. All of the models of neuronal activity tested in this experiment returned relatively low R^2 values. The best performing model returned R^2 values that were typically below 0.4. However, these low R^2 values should not be interpreted as weak statistical support for the models. The expected R^2 values will depend to some extent on the design of the experiment.

To illustrate this point, imagine recording from a visually responsive neuron in V1 that responds well to a line segment and is tuned to orientation, direction of motion, speed, length of stimulus, the eye through which the stimulus is presented, and the luminance contrast of the stimulus. Imagine testing the neuron with a set of stimuli that vary only in orientation. No other stimulus attribute is varied. Under this condition, the firing rate of the neuron will vary from trial to trial, and the variance will be largely attributable to the orientation of the stimulus. A regression against orientation should return a high R^2 value, perhaps as high as 90%. This is because all other sources of variance have been minimized. Such an experiment asks whether orientation tuning, when isolated, is statistically reliable.

However, now imagine testing the neuron with a stimulus set in which all parameters are free to vary. From trial to trial, the stimulus changes in orientation, direction of motion, speed, length, the eye through which the stimulus is presented, and luminance contrast. The firing rate of the neuron will vary from trial to trial, but now the variance will arise from many sources. A regression against orientation should return a low R^2 value, perhaps in the 20–40% range, because orientation will account for only one part of the total variance. This seemingly low R^2 value, however, would not indicate a lack of orientation tuning, or a miminal or unimportant orientation tuning. Rather, it would indicate that orientation tuning accounts for a piece of the total variance, and that other factors must account for the remainder of the variance. One would expect the regression on orientation, even with a "low" R^2 of 0.2, to be highly statistically significant. This experimental design asks, in a varied stimulus set, (*i*) whether orientation tuning makes a

statistically significant contribution, and (*ii*) what proportion of the total variance of the neuron stems from orientation tuning.

In the same manner, in the present experiment we tested (*i*) whether each model of motor tuning made a statistically significant contribution to the pattern of firing of the neuron, and (*ii*) how much of the total variance of the neuron stemmed from each model. For example, one neuron, when tested on the end-posture-tuning model, returned an R^2 value of 0.38. The regression was highly significant ($P < 0.0001$). In this example, (*i*) end-posture tuning made a significant contribution to the behavior of the neuron, and (*ii*) 38% of the variance in the neuron's firing could be attributed to end-posture tuning, whereas the remainder of the variance must have been driven by other factors. Given the design of the experiment (the inclusion of an unrestricted, naturalistic movement set), such low R^2 values are expected. Particular attention, therefore, must be paid to the associated P value to ascertain the statistical significance of the fit.

Measurement of Joint Angles. The positions of points on the limb were measured by means of an Optotrak 3020 system (Northern Digital). This system tracks the 3D position of infrared light emitting diodes (LEDs). Each LED could be separately tracked to a spatial resolution of 0.1 mm. The position was measured every 14.3 ms. To create a marker that could be detected by the Optotrak cameras from any angle, we glued five individual LEDs together to produce an omni-directional marker ball. A marker ball was taped to the monkey's forefinger on the dorsal surface where it would not interfere with grasping; on the thumb, again on the dorsal surface where it would not interfere with grasping; on the back of the hand, between the knuckles of the third and fourth digits; and on the lateral aspect of the elbow. In addition, 14 individual markers were taped in a double ring around the monkey's wrist, with seven markers per ring and a 1-cm spacing between the rings. The wires were taped in a bundle to the underside of the arm and draped behind the monkey. The primate chair was open at the front and side, allowing for almost total range of movement of the arm. The monkey's other arm, ipsilateral to the electrode, was not studied with Optotrak markers. To ensure that this hand would not

reach for the fruit rewards during trials, or tear off the markers taped to the measured hand, this untested hand was fixed to the side of the chair in an arm holder.

The double ring of 14 markers around the wrist was subject to a rigid body computation to calculate the location and spatial orientation of the wrist. In this computation, for each time point, a 3D rigid model of the double ring of markers was fitted to the measured positions of the currently visible markers, using a least-squares method of optimal fit. The orientation and position of the model could then be used to estimate the orientation and center of the wrist. The center of the wrist was taken to be the mean position of the 14 points in the model.

The position of the shoulder in space was calculated by analyzing the position of the elbow over time. Over many time points, the elbow described a portion of a sphere, the origin of which was located at the shoulder joint. For each 3 min block of data, a shoulder position was calculated by fitting a sphere to the data using a least-squares best fit algorithm and using the center of the sphere as the shoulder location. Because the shoulder is capable of small translational movements in addition to rotations, this method of estimating shoulder joint location is approximate but was sufficient for the purposes of this study. When the shoulder position was calculated multiple times over different time segments, it varied within <3 cm.

Three shoulder angles were computed: the elevation; the azimuth; and the "twist" or internal/external rotation of the shoulder joint. We also calculated the flexion of the elbow; the pronation of the forearm; the extension of the wrist; the adduction of the wrist; and the grip aperture. In total, eight degrees of freedom were calculated for the arm. This model of the arm was verified by applying forward kinematics to estimate the position of the hand. This calculated position of the hand matched the actual, measured position of the hand to within an accuracy of 1.5 cm.

Description of Movements in the Data Set. During testing of a neuron the monkey was allowed to move its contralateral arm freely to touch and explore parts of the primate

chair, to reach for small pieces of fruit held out on the end of forceps, to bring food to its mouth, to retrieve food from its mouth, to hold food in central space to examine it, and to rotate and explore food items. Occasionally the monkey also scratched at its skin or scratched rhythmically at a portion of the monkey chair. The movement of the arm was recorded through all of these behaviors. Different types of behaviors were not separated in the analysis, partly because one type of behavior tended to grade into another type and the distinction could only be made subjectively; and partly because the purpose of the study was to include all possible arm movements in as large and naturalistic a range as possible given the constraints of the primate chair.

For each neuron, the position of the hand in 3D space was tracked during a continuous time interval ranging from 10 to 30 min. Separate movements were extracted from this data set on the basis of a velocity analysis. Minima in the velocity were identified and the intervals between minima were flagged as potential separate movements. To enter the final data set, the movement had to be at least 0.15 sec in duration and the peak speed had to be at least 20 cm per sec. These parameters seemed to successfully divide the data into discrete segments that matched our subjective impression of separate hand movements.

Fig. 4 shows a typical movement set collected during testing of a neuron. This set shows 683 separated movement segments that densely sampled the workspace of the hand. Vertically, the movements ranged from 29 cm below the mouth to 9 cm above the mouth. Horizontally the movements ranged on the contralateral side (same side as the studied arm, opposite side as the electrode) to 19 cm from the midline, and on the ipsilateral side to 13 cm from the midline. In depth (direction along the monkey's forward line of sight) the movements ranged from 5 cm behind the level of the mouth (such as when the monkey was reaching to its flank or to its ear) out to 21 cm in front of the mouth (normal for a fully extended reach).

The average length of a movement was 9 cm (SD 6.6). The average hand speed was 26.7 cm/sec (SD 13.5). Each movement had a peak speed, and the average peak speed among all movements was 46.2 cm/sec (SD 28.1).

For each movement we calculated a standard curvature metric, as follows. The straight-line distance between the start and end of the movement was found. The total path-length of the movement was found. The ratio of these two quantities provided a curvature metric in which 1.0 corresponds to no curvature and smaller numbers correspond to increasingly curved movements. The average curvature was 0.9 (SD 0.08), indicating that the movements tended to be straight. In the figure, some movements appear to be highly curved. This appearance is a result of collapsing a 3D movement into a 2D depiction in which the long axis of the movement is not fully shown.

The distribution of movement directions was examined. For each movement we calculated a direction by connecting the start point to the end point and obtaining the azimuth and elevation angles. These directions were then plotted on a sphere. The directions appeared to be relatively evenly distributed. The sphere was divided into 20 equal sectors, and the movement directions were distributed over these 20 sectors with all sectors represented.

Preliminary Analysis of Neurons. To further specify the somatotopic portion of motor cortex that was studied, we performed a preliminary analysis on each neuron. Using a step-wise regression, we obtained the degree of correlation between the neuronal activity and the velocity of each of the eight measured joints. If we were recording primarily in a distal representation, we would expect to find significant regressions with distal joints including hand aperture, wrist flexion, wrist adduction, and forearm pronation. If we were recording primarily in a proximal representation, we would expect to find significant regressions with promixal joints including elbow flexion and the three degrees of shoulder rotation. Given the known overlap in motor cortex somatotopy, we expected to find intermingled neurons related to both proximal and distal joints. The results indicated that 89% of the neurons were significantly related to the proximal joints and 67% were significantly related to the distal joints. These results indicate that the studied neurons were in the forelimb representation in a region that emphasized the proximal joints over the distal joints.

Direction Tuning. Each neuron was tested for direction tuning in the following manner. For each movement, we calculated a mean firing rate of the neuron (spikes per sec during the movement). Since the neuron was presumed to affect movement with a conduction latency and a latency caused by the inertia of the arm, we shifted the analysis window for the single neuron data with respect to the movement data by a specific temporal offset. The appropriate offset for each neuron was estimated from the electrical stimulation data from the same cortical site, and was the latency for the hand to move after onset of electrical stimulation. This latency was typically about 70 ms.

Each hand movement was assigned a direction in Cartesian space based on the vector connecting the beginning and end point of the movement. Firing rate was modeled as a function of the angular deviation ($\Delta\theta$) between this movement vector and a preferred direction.

Firing rate = A cos ($\Delta\theta$) + B.

A regression analysis was used to find the optimal preferred direction and coefficients, following the method of Georgopoulos *et al.* (1). The regression analysis provided an R^2 value indicating how much of the variance in neuronal activity could be attributed to the direction-tuning model. The regression analysis also provided an F and P value indicating whether the data showed a statistically significant trend in the direction of the model.

End-Point Tuning. For this model of neuronal tuning all data concerning the direction or trajectory of the movement was discarded and only the end-point of the movement was considered. Firing rate was modeled as a Gaussian function of these end-points in Cartesian space. In the following equation, $x1$, $x2$, and $x3$ refer to the three Cartesian coordinates of the end-point of the movement; $P1$, $P2$, and $P3$ refer to the coordinates of the peak of the Gaussian; the standard deviations of the Gaussian around that peak are indicated by $\sigma1$, $\sigma2$, and $\sigma3$; the height of the Gaussian at peak is given by A; and the height of the Gaussian at lowest, or the estimated baseline firing rate of the neuron, is B.

A nonlinear regression technique (2) was used to fit this equation to the data for each neuron.

$$\text{Firing rate} = Ae^{\frac{(x_1-P_1)^2}{2\sigma_1{}^2}+\frac{(x_2-P_2)^2}{2\sigma_2{}^2}+\frac{(x_3-P_3)^2}{2\sigma_3{}^2}} + B$$

End-Posture Tuning. This model followed the same general equation as the previous model except that it involved the eight dimensions of arm posture space ($x1$ through $x8$) rather than the three dimensions of Cartesian space. Firing rate was modeled as a Gaussian function that had a peak at a specific, preferred posture. Again a non-linear regression technique was used to fit the model to the data for each neuron.

$$\text{Firing rate} = Ae^{\sum\limits_{i=1:8}\frac{(x_i-P_i)^2}{2\sigma_i{}^2}} + B$$

End-Posture Plus Trajectory. This model added a term to the end-posture model. The movement of the arm through posture space was assigned an 8D vector that connected the beginning posture to the end posture of the movement. A second vector was defined connecting the beginning posture of the movement to the estimated preferred posture of the neuron. The angular deviation $\Delta\theta$ was defined as the difference in angle between these two vectors. In this model:

$$\text{Firing rate} = (C\cos(\Delta\theta) + D)(Ae^{\sum\limits_{i=1:8}\frac{(x_i-P_i)^2}{2\sigma_i{}^2}} + B)$$

Testing Artificial Neurons. To test the validity of the above regression models, we generated artificial neurons. One artificial neuron was direction tuned. To generate the neuron we used the hand movements of an actual data set, but replaced the firing-rate data with artificially generated data. The data were generated using the direction-tuning

model, and then randomized noise was added to create a neuron that was noisily tuned to a preferred direction. The neuron was then subjected to the regression analyses described above. Fig. 5*A* shows the result. When tested with a direction-tuned model, the artificial direction tuned neuron showed a mid-range R^2 value consistent with its noisy tuning. When tested with the other regression models, it showed near zero R^2 values.

In a similar manner we generated an artificial neuron that was tuned to a final hand location in space, and an artificial neuron that was tuned to a final posture of the arm. The results, shown in Fig. 5 *B* and *C*, show that the R^2 value for each type of neuron was highest for the matching type of regression model and near zero for the non-matching regression models. These tests indicate that the regression models were successful at distinguishing neurons that had different types of tuning, with relatively little cross-contamination between the different regression models.

Distribution of Joint Angles Preferred by End-Posture-Tuned Neurons. For each neuron recorded from motor cortex, we used the end-posture regression model to obtain a Gaussian fit to the data in 8D posture space. We then examined the distribution of preferred end-postures among neurons. Not all neurons were sharply tuned in posture space. To examine the distribution of those neurons that had clear preferred postures, we ranked neurons by the sharpness of the Gaussian tuning function and arbitrarily chose the 50% of neurons that were most sharply peaked, thus the neurons for which the end posture was most clearly specified. These neurons are represented in Fig. 6. Each frequency histogram shows data for one joint. For most joints, neurons were tuned to a range of different preferred angles. For some joints, especially distal joints, neurons were more likely to be tuned to an extreme angle. Neurons tended to prefer a closed grip aperture.

1. Georgopoulos, A. P., Schwartz, A. B. & Kettner, R. E. (1986) *Science* **233,** 1416-1419.

2. Cohen, J., Cohen, P., West, S. G. & Aiken, L. S. (2003) *Applied Multiple Regression/Correlation Analysis for the Behavioral Sciences* (Lawrence Erlbaum Associates, Mahwah, NJ), 3rd Ed.

Figure Legends for Supporting Online Material

Figure 4 (Figure 1 supplemental): Front view of 683 hand movements made during 15 min. Each trail of dots = 1 movement measured at 14.3 ms intervals. Monkey drawing shows approximate scale and location of animal.

Figure 5 (Figure 2 supplemental): Analysis of artificially generated, noisy neurons. A. Artificial direction-tuned neuron tested on direction, end-point, and end-posture regression models. B. Artificial end-point tuned neuron tested on the same three models. C. Artificial end-posture tuned neuron tested on the same three models.

Figure 6 (Figure 3 supplemental): Distribution of end postures preferred by neurons. Each graph shows a frequency histogram for neurons that preferred specific values for joint angle and grip aperture.
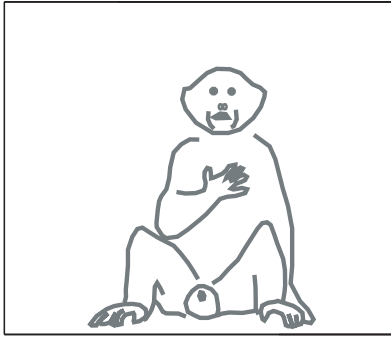
Figure 1
1 column
Supplemental materials
Aflalo & Graziano

A   Direction-tuned artificial neuron

Regression Model:
■ Direction
■ End-point
■ End-posture

R^2

B   End-point-tuned artificial neuron

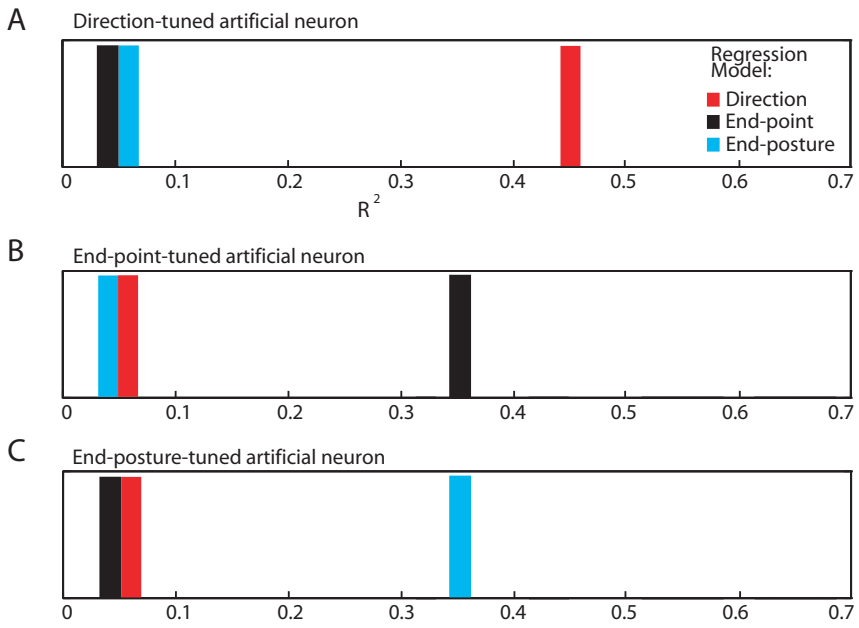C   End-posture-tuned artificial neuron
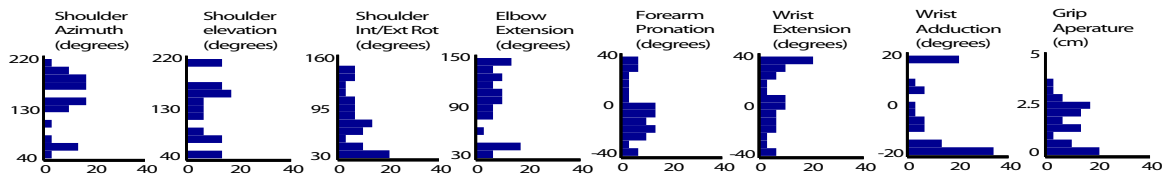
Figure 2
2 Columns
Supplemental Materials
Aflalo & Graziano

Figure 3
2 columns
Supplemental materials
Aflalo & Graziano